Complement Protein C9 Labeled with Fluorescein Isothiocyanate Can Be Used To Monitor C9 Polymerization and Formation of the Cytolytic Membrane Lesion†

Peter Jay Sims

ABSTRACT: Human complement protein C9 was covalently labeled with the fluorescent chromophore fluorescein isothiocyanate (FITC) with only a small reduction in the cytolytic activity of the protein. Polymerization of the labeled protein—either by incubating with lipid vesicles treated with complement proteins C5b-8 (activating the C5b-9 membrane lesion) or by heating the protein [Tschopp, J., Muller-Eberhard, H. J., & Podack, E. R. (1982) *Nature* (*London*) *298*, 534]—resulted in a 40–60% decrease in the fluorescence emission from FITC. The decrease in total fluorescence was accompanied by an increase in the steady-state anisotropy following activation and polymerization of FITC-C9 by C5b-8 membranes, while heat-induced aggregation of the protein resulted in a dramatic depolarization of fluorescence. Only small changes in either the absorbance spectrum or fluorescence lifetime of the chromophore were detected upon FITC-C9 polymerization. Evidence is presented that the measured changes in FITC fluorescence upon C9 activation are due to self energy transfer between closely apposed fluorescein chromophores which occur in the polymerized form of the protein. The significance of these observations to the molecular structure of the assembled C5b-9 complex is discussed, as are the potential applications of this fluorescent derivative of C9.

The cytolytic membrane lesion of the serum complement system is initiated upon the association of component C9 with membrane-bound complexes formed by complement proteins C5b6, C7, and C8 (Muller-Eberhard, 1975; Mayer, 1972; Esser, 1981).[1] Recent evidence suggests that the interaction of C9 with the C5b-8 complex on the membrane surface (MC5b-8) results in the polymerization of multiple molecules of C9 into an annulus-ringed cylindrical structure that embeds into the membrane (Podack & Tschopp, 1982a,b; Podack et al., 1982; Tschopp et al., 1982a). It has been proposed that the MC5b-8-initiated polymerization of C9 is integral to the expression of hydrophobic domains within the molecule, which then intercalate through bilayer lipid to initiate functional membrane damage and consequent cell death (Tschopp et al., 1982a). The bilayer-disordering and channel-forming properties of the membrane-bound C5b-9 proteins have been the subject of extensive investigation (Michaels et al., 1976; Sims & Lauf, 1978; Esser et al., 1979; Ramm et al., 1982a,b).

Support for a model of membrane damage by polymerized complexes of C9 derives from the ultrastructural identity of the C9 polymer with the doughnut-ringlike structures known to be formed by the complement proteins on membrane surfaces, as well as from direct biochemical demonstration of the aggregation of C9 into detergent-resistant complexes with an apparent molecular weight of 10^6 that have been shown to form upon incubation of C9 with C5b-8 treated membranes or spontaneously upon heating or chemical denaturation of the molecule (Dourmashkin, 1978; Bhakdi & Tranum-Jensen, 1978; Podack & Tschopp, 1982a,b; Tschopp et al., 1982a; Yamamoto & Migita, 1983).

Although considerable information pertaining to the molecular events which occur at the site of the C5b-9 membrane lesion have been derived from ultrastructural studies of the proteins in situ, and from biochemical studies performed on detergent-extracted C5b-9 complexes, direct real-time observation of the molecular events which occur during the interaction of these five proteins on membrane surfaces has for the most part been precluded by the number and complexity of the proteins that interact to initiate the membrane lesion. Since the covalent labeling of membrane-associated and other complex multimeric proteins with fluorescent reporter groups has proven to be a valuable tool in the study of dynamic protein–protein and protein–lipid interactions, we have undertaken to label the cytolytic complement proteins with fluorescent chromophores suitable for direct spectroscopic observation of the dynamics of the molecules in situ, during their activation and insertion into biological membranes.

We report here on the functional, biochemical, and spectroscopic properties of a fluoresceinated derivative of complement protein C9 (FITC-C9)[2] and describe the mechanisms by which the steady-state fluorescence emission of this probe is altered upon the formation of aggregated complexes of the protein. We also discuss how this probe can be used to measure the kinetics of C9 activation and polymerization on lipid vesicle and cell membrane surfaces that have been treated with complement proteins C5b-8. A detailed analysis of the kinetics and temperature dependence of FITC-C9 polymerization by MC5b-8 is described elsewhere (Sims & Wiedmer, 1984).

Materials and Methods

Materials. Fluorescein 5-isothiocyanate (FITC; isomer I) was obtained from Molecular Probes. $Na^{125}I$ was obtained in dilute carrier solution from Amersham. Egg phosphati-

† From the Immunohematology Laboratory, the Department of Pathology and the Department of Biochemistry, University of Virginia Medical School, Charlottesville, Virginia 22908. *Received September 27, 1983.* This research was supported by a grant-in-aid from the American Heart Association with funds contributed in part by the Virginia Affiliate and by a grant from the Thomas F. Jeffress and Kate Miller Jeffress Memorial Trust. P.J.S. is a John A. Hartford Fellow.

[1] Complement proteins are named in accordance with recommendations of *Bull. W. H. O.* (1968). The prefix "M" (e.g., MC5b-8) is used to indicate that the protein is membrane bound.

[2] Abbreviations: FITC, fluorescein 5-isothiocyanate; BSA, bovine serum albumin; EDTA, ethylenediaminetetraacetic acid; TES, 2-[[tris(hydroxymethyl)methyl]amino]ethanesulfonic acid; SRBC, sheep red blood cells; CH_{50}, the amount of protein exhibiting 50% of maximal hemolytic activity; SDS, sodium dodecyl sulfate; PAGE, polyacrylamide gel electrophoresis; RET, resonance energy transfer.

0006-2960/84/0423-3248$01.50/0

dylcholine was obtained in chloroform from Avanti Polar Lipids. Triton and TES were obtained from Calbiochem-Behring, Corp. Human IgG, fatty acid free bovine serum albumin, oyster glycogen type 2, and Ficoll 70 were each obtained from Sigma. Rhodamine B and Me_2POPOP, 1,4-bis(4-methyl-5-phenyloxazol-2-yl)benzene were obtained from Aldrich. Horse spleen ferritin (electron microscopy grade) was from Polysciences. All chemicals were of analytical grade, and all organic solvents were of spectroscopic grade.

Solutions. All solutions were freshly prepared with H_2O obtained by reverse osmosis and ultrafiltration (Millipore, Boston, MA). Except where indicated otherwise, all reagents contained 0.02% (w/v) NaN_3: *buffer I*, 150 mM NaCl–10 mM TES, pH 7.50. *GVBS*, 0.1% (w/v) gelatin in 150 mM NaCl–3.3 mM sodium barbital, pH 7.40. *GVBE*, GVBS made in 10 mM EDTA.

Complement Proteins. Human complement proteins C5b6, C7, and C8 were purified and assayed for functional (hemolytic) and membrane-binding activity according to methods previously described (Sims, 1983). C9 was purified from freshly drawn human serum by sequential chromatography on DEAE-Sephacel (Pharmacia), HA-Ultrogel (LKB), and Sephacryl S-200 (Pharmacia) according to published methods (Biesecker & Muller-Eberhard, 1980; Hammer et al., 1981; Ishida et al., 1982). The hemolytic and membrane-binding activities of C9 (and labeled derivatives of C9) were assayed according to methods described below. C5b6 was stored at −20 °C in 250 mM NaCl, 10 mM TES, and 1 mM EDTA (pH 7.50) containing 40% (w/v) glycerol. C7, C8, and C9 were stored at −20 °C in buffer I containing 40% (w/v) glycerol.

Immediately before use, all proteins were dialyzed and concentrated against buffer I (Microprodicon Model MPDC-120, Biomolecular Dynamics). Prior to labeling with ^{125}I or FITC, C9 was routinely rechromatographed on Sephacryl S-200 (1.6 × 90 cm) to remove high molecular weight aggregates frequently found to form spontaneously during storage.

Immunochemical Procedures. Goat antiserum against human complement protein C9 used in these studies was produced by subcutaneous injection of 3 mg of C9 suspended in Freunds complete adjuvant (priming dose) followed by two secondary intramuscular injections of 2 mg of C9 suspended in Freunds incomplete adjuvant at intervals of 14 days. Eight days after boosting, serum was obtained by phlebotomy. The IgG fraction of the antiserum was prepared by affinity chromatography on DEAE Affi-Gel Blue (Bio-Rad), followed by precipitation with 50% ammonium sulfate.

C9 used in this study was analyzed on Ouchterlony plates (Ouchterlony, 1968) with 0.5–10 μg of the antigen tested against goat antiserum raised against the protein (above) and commercial antisera produced against human serum albumin (rabbit; Cappell), human IgG (goat; Atlantic Antibodies), human C7 (goat; Miles), human C8 (goat; Miles), and whole human serum (goat; Meloy). Plates were analyzed at 24, 48, and 72 h.

Radiolabeling. Radioiodination of C9 was performed in azide-free phosphate-buffered saline at 0 °C by using the solid-phase glucose oxidase–lactoperoxidase system (Enzymobeads; Bio-Rad). Unreacted label was removed by chromatography on Sephadex G-25 (PD-10; Pharmacia). Albumin was added to 2% (w/v). Specific activities of (0.1–2) × 10^6 cpm/μg of protein were achieved.

FITC Labeling of C9 (FITC-C9). Labeling of C9 with fluorescein isothiocyanate (FITC) was performed at pH 8.70 in 150 mM NaCl–50 mM sodium carbonate, by incubation in the dark at 0–2 °C, for 6–12 h. FITC was delivered to C9 (0.5–1 mg/mL protein in sodium carbonate buffer) with rapid stirring as a 100 or 10 mM stock solution in dimethylformamide. The input of FITC was varied between 10:1 and 200:1 on a molar basis to achieve final dye/protein ratios of from 0.3 to 2. Final concentration of carrier solvent in the reaction bath never exceeded 3% (v/v). Following incubation, unreacted label was removed by chromatography in buffer I (Sephadex G-25, PD-10; Pharmacia) followed by a 24-h dialysis against 3 × 2 L of the same buffer (performed in the dark at 2 °C). When necessary, FITC-C9 was rechromatographed (after labeling) on Sephacryl S-200 (0.9 × 60 cm) to remove trace aggregates of the protein spontaneously formed during labeling. Until used, labeled proteins were kept in the dark at 2 °C as 0.1–0.5 mg/mL solutions in buffer I.

Determination of Protein Concentrations and Dye/Protein Ratios. Protein concentrations were determined from the absorbance measured at 280 nm (A_{280}) by using extinction coefficients of $\epsilon = 0.99$ (C7), $\epsilon = 1.6$ (C8), and $\epsilon = 0.96$ (C9) mL mg^{-1} cm^{-1} (Podack & Tschopp, 1982a). Molecular weights of 124 000 (C7), 151 000 (C8), and 71 000 (C9) were employed to determine molar concentrations. Because of the strong UV absorbance of FITC conjugated to the protein, the protein concentrations of FITC-C9 solutions were determined by dye-binding assay (Bio-Rad) using known solutions of unlabeled C9 in buffer I (concentrations determined from A_{280}) as concentration standards.

Molar quantities of bound FITC were determined from the absorbance at 495 nm, on the basis of a molar extinction coefficient of 60 000 M^{-1} cm^{-1} for covalently bound FITC in buffer I at 23 °C, pH 7.5, as determined according to methods described by Wang & Taylor (1980).

Hemolytic Assay. The cytolytic activity of FITC-C9 toward complement-treated sheep red blood cells (SRBC) was routinely measured in a standard hemolytic assay: 2.5 × 10^9 SRBC were made C5b67 by rapid mixing with C5b6 and C7 (530 μg added sequentially) in a total volume of 2.5 mL of GVBS. Following incubation (15 min, 37 °C), the cells were washed and suspended to 4.4 × 10^8/mL in the same buffer. Aliquots of 25 μL of the C5b67 SRBC (1.1 × 10^7 cells were then suspended with 25 ng of C8 and various quantities of C9 (or FITC-C9) in a total volume of 75 μL of GVBE; 1.1 × 10^7 C5b67 SRBC in 75 μL of GVBE or 75 μL of H_2O served as 0% and 100% hemolysis controls, respectively. Following a 30-min incubation at 37 °C, 2 mL of ice-cold GVBE was added, the tubes were centrifuged (15 min, 1300*g*, Sorvall RT6000), and the supernatants were recovered. Percent hemolysis was determined spectrophotometrically from the absorbance measured at 412 nm. The C9 (or FITC-C9) input resulting in 50% cell hemolysis (CH_{50}) was determined graphically and comparison made to the C9 hemolytic activity of normal pooled human serum, assuming a normal serum C9 concentration of 58 μg/mL (Biesecker & Muller-Eberhard, 1980). By this assay, serum C9, and purified C9 used for labeling, exhibits a specific activity of 1.8–2.0 CH_{50}/ng. The CH_{50} values of various preparations of FITC-C9 were found to range between 1.3 and 2.5 CH_{50}/ng, suggesting that the FITC-C9 retains greater than 65% of the hemolytic activity of the unlabeled protein.

Polyacrylamide Gel Electrophoresis (PAGE). Unlabeled complement proteins and FITC-C9 were analyzed by PAGE according to the procedures of Laemmli (1970). Proteins were denatured by heating (5 min, 100 °C) in 10% sodium dodecyl sulfate (SDS) under nonreducing conditions and applied to

tube gels formed of 7% acrylamide (4% acrylamide stacking gel). Following electrophoresis, the protein bands were visualized by staining with Coomassie. Staining was quantitated by densitometry at 545 nm (Quick Scan; Helena Laboratories). In the case of FITC-C9, duplicate gels (unstained) were sliced into 6-mm segments and extracted with 0.5 mL of 1% Triton (Jackson et al., 1983). Following dilution to 2.5 mL final volume with buffer I, and centrifugation (30 min, 1300*g*, Sorvall RT6000) to remove gel pieces, the fluorescence of the Triton-extracted material from each gel segment was measured with excitation at 470 nm and emission at 520 nm.

Heat-Induced Aggregation of FITC-C9. The polymerization of FITC-C9 was induced by incubation at 52 °C for either 2 or 3 h (Podack & Tschopp, 1982a,b; Tschopp et al., 1982a). Stock solutions (0.02–5 μM) of FITC-C9 were prepared in buffer I and divided, 2.5 mL was placed in a light-shielded heating block at 52 °C, and the remainder was stored in the dark at 2 °C. Following incubation, absorbance and fluorescence spectra were obtained and steady-state fluorescence anisotropies and fluorescence lifetimes determined for both heated samples and controls. All optical measurements were made with samples equilibrated at 23 °C. Light scattering was estimated from samples of C9 (unlabeled) incubated under conditions identical with those used for FITC-C9. Following spectroscopy, samples were saved for analysis by electron microscopy and molecular sieve chromatography.

Molecular Sieve Chromatography of Monomeric and Heat-Polymerized FITC-C9. Molecular sieve chromatography on Sephacryl S-300 (Pharmacia) was used to demonstrate conversion of the FITC-C9 monomer to a high molecular weight polymer upon heating. Monomeric FITC-C9 and FITC-C9 incubated at 52 °C as described above were each applied (300 μg in 0.5 mL) to a 0.9 × 60 cm column of Sephacryl S-300 equilibrated with buffer I at 2 °C. Flow rate was 2.2 mL/h, and 1-mL fractions were collected. Absorbance due to protein (at 280 nm) and fluorescence due to FITC (emission 520 nm; excitation 470 nm) of each fraction were measured. Absorbance measurements were made on the undiluted samples, and fluorescence was measured after dilution to 3 mL in buffer I. Molecular weights were estimated by comparison to marker proteins IgM (M_r 950000), ferritin (M_r 460000), and bovine serum albumin (M_r 67000). Void volume (V_0) was determined with blue dextran 2000 (Pharmacia).

Preparation of Large Unilamellar Vesicles (LUV). Large unilamellar vesicles (LUV) were formed of egg phosphatidylcholine by the reverse-phase evaporation method (Duzgunes et al., 1983; Szoka & Papahadjopoulos, 1978). Chloroform was removed from 15 mg of lipid by evaporation under a stream of N_2, and the lipid was maintained under <5 torr for 12–16 h. The lipid was dissolved in diethyl ether (3 mL), then mixed with 1 mL of buffer I, and sonicated at 30 °C in a bath sonicator (Heat Systems–Ultrasonics Model 375W) maintained under N_2. The ether was then slowly removed by rotary evaporation under slight vacuum. Aggregated lipid was removed by centrifugation (5 min, 833*g*, Sorvall RT6000), and the resulting vesicles were used without further fractionation. Vesicles were stored at 2 °C as a 9.3 mg/mL stock suspension for use up to 10 days. Examination by freeze–etch electron microscopy revealed that >95% of the resulting vesicles were single chambered (unilamellar), with vesicle size ranging between 50- and 1000-nm diameter.

Assembly of MC5b-9 Complex. The membrane-bound C5b-9 complex (MC5b-9) was assembled on LUV by sequential incubation with the purified proteins C5b6 + C7 (to generate membrane-bound C5b67 complexes) followed by addition of C8 and C9 (or FITC-C9). Typically, C5b67 LUV were prepared by mixing the vesicles (9.3 mg/mL of lipid) with C5b6, followed by the addition of C7 at molar equivalence to C5b6 (1 mg of protein/9.3 mg of lipid). After immediate mixing, the vesicle suspension (final lipid concentration 3.1 mg/mL) was incubated 15 min at 37 °C and then placed on ice. LUV (3.1 mg/mL of lipid) not exposed to C5b6 + C7 (or LUV exposed to C5b6 but not C7) served as controls. For some experiments, C5b67 LUV were isolated from unbound proteins by floatation on a discontinuous Ficoll 70 density gradient (see below). MC5b-9 was assembled by the addition of C8 (0–20 μg of protein/155 μg of lipid) and FITC-C9 (0–20 μg of protein/155 μg of lipid) at 30 °C (or a temperature as otherwise noted) to preformed C5b67 LUV. In certain experiments, ^{125}I-C9 or unlabeled C9 substituted for FITC-C9. For fluorescence measurements, FITC-C9 (0–20 μg) was generally suspended with C5b67 or control LUV (155 μg lipid in a final volume of 2.1 mL) in a stirred cuvette before the addition of C8, in order to record initial monomer fluorescence prior to MC5b-9 assembly; C9 binding and polymerization were then activated by the addition of C8 (0–20 μg of protein delivered as a 1 mg/mL solution in buffer I) and incubation at 30 °C.

Density Gradient Floatation of LUV. To separate C5b67 and C5b-9 (FITC-C9 and/or ^{125}I-C9) LUV from unbound protein, vesicles were floated through discontinuous density gradients of Ficoll 70 in buffer I by a modification of procedures described by Hu et al. (1981). Vesicles (C5b-9, C5b67, or controls) were mixed with 40% (w/v) Ficoll 70 (final Ficoll concentration 28% in 1.0 mL) in 0.5 × 2 in. centrifuge tubes and overlayed with 1.5 mL each of 20% and 15% (w/v) Ficoll. The gradient was then overlayed with 0.5 mL of buffer I. The tubes were centrifuged (60 min, 45000 rpm) in a Beckman SW65 rotor at 2 °C. The tubes were punctured from the bottom and the contents chased with 50% (w/v) sucrose. Fractions of 300 μL were collected (ISCO Model 185 density gradient fractionator) and assayed for fluorescence, radioactivity, and phosphate. For certain experiments, similar gradients of 400 μL total volume were prepared in 5 × 20 mm tubes and then centrifuged for 60 min at 80000*g* (Beckman airfuge). The visible lipid band at the buffer/Ficoll interface was recovered by aspiration into a pipet.

Radioactivity of samples was measured by γ counting in a Beckman 4000. Phosphate was determined by the method of Bartlett (1959).

Electron Microscopy. Samples were examined by freeze–etch and negative-stain electron microscopy with a Hitachi HU12A at 75 kV. Freeze–etch replicas were prepared with a Balzers BAF 300. Negative staining was performed with 1% phosphotungstic acid. The dried grids were generally examined at 90000X magnification and bright field image photographed with Kodak S0-163 film.

Absorbance Spectroscopy. Dual-beam absorbance measurements were made in 1-cm path-length quartz cuvettes by using either a Beckman Model 35 spectrophotometer or a Hewlett-Packard Model 8450A diode-array spectrophotometer. Throughout, samples were equilibrated at 23 °C.

Fluorescence Spectroscopy. All fluorescence measurements were obtained with a SLM4800S spectrofluorometer equipped for sample stirring and temperature control. Excitation was provided by an Osram 450-W xenon arc lamp and emission detected by Hamamatsu R928P photomultiplier tubes. Wavelength selection was provided by single grating monochromators (excitation and emission). For certain measurements, a cutoff filter (Schott 0G515), fused silica glass neutral

density filters (Melles-Griot), and calcite prism polarizers (Glan-Thompson) were added. To reduce photobleaching, shutters were closed except during data acquisition; 1-cm path-length quartz cuvettes containing 2–3 mL volume of samples were employed throughout. Provision was made for addition to the stirred sample by injection (Hamilton syringe) through a light-tight port above the sample compartment.

All spectra were recorded as a ratio to the emission from 3 g/L rhodamine B in ethylene glycol, contained in a front surface cuvette placed in the reference compartment. A Schott RG630 filter was placed before the reference channel photomultiplier tube. Unless otherwise indicated, excitation spectra were recorded with an excitation bandwidth of 1 nm, and the emission monochromator was set at 540-nm (8-nm slits). For emission spectra, a 1 nm emission bandwidth was employed. All emission spectra were corrected for the wavelength-dependent response of the photomultiplier tubes by using correction factors obtained by NBS lamp calibration supplied by the manufacturer. Where necessary, correction was also made for light scattering from vesicles (or protein), which was determined from identical suspensions containing unlabeled C9 substituted for FITC-C9. Except where otherwise indicated in the text, all fluorescence measurements were made with samples equilibrated at 23 °C.

Quantum yields (ϕ)[3] were derived for FITC-C9 (excitation at 495 nm) from the corrected emission spectra (integrated from 470 to 650 nm in 2-nm steps) by using sodium fluorescein in 0.1 N NaOH as a reference quantum standard ($\phi_R = 0.85$ for excitation at 490 nm; Chen, 1969). Excitation and emission polarizers were set at 0° (vertical) and 54.7°, respectively, to correct for polarized emission from FITC-C9 (Spencer, 1970; Shinitzky, 1972). To minimize inner filter effects, optical densities of measured solutions (at peak absorbance wavelengths) were always less than 0.05. Correction for the difference in lamp output at 490 nm (excitation for sodium fluorescein) vs. 495 nm (excitation for FITC-C9) was made by ratioing sample fluorescence to the emission from rhodamine B placed in the reference compartment as described above.

Samples quantum yields (ϕ_S) were calculated according to eq 1 where $\int F_S$ and $\int F_R$ are the integrated areas under the

$$\phi_S = (0.85)\frac{A_R \int F_S}{A_S \int F_R} \quad (1)$$

corrected emission spectra of the sample and fluorescein reference solution, respectively, and A_S and A_R are the absorbances measured for the sample and fluorescein reference solutions at the excitation wavelengths (495 and 490 nm, respectively).

Steady-State Fluorescence Anisotropy. Steady-state fluorescence anisotropy (r) was determined by measurement of the ratio of the parallel (I_{VV}) to perpendicular (I_{VH}) components of emission using vertically polarized exciting light. Excitation of 470 nm (4-nm bandwidth) was employed. Fluorescence was recorded through two emission monochromators each set at 520 nm (4-nm slits) which were arranged in T format. To correct for the differential response of the two channels to vertical and horizontal components of emission, the ratio (I_{HV}/I_{HH}) was determined by using horizontally polarized excitation. Anisotropy (r) was normally calculated according to eq 2. For samples exhibiting measureable light

$$r = \frac{(I_{VV}/I_{VH})(I_{HH}/I_{HV}) - 1}{(I_{VV}/I_{VH})(I_{HH}/I_{HV}) + 2} \quad (2)$$

scattering (e.g., LUV suspensions), correction was made for the scattered contribution to each component of the polarized emission I_{VV} and I_{VH} according to methods described by Shinitzky et al. (1971). The suitability of this correction (to within experimental error) was confirmed by sample dilution (data not shown) as suggested by Lakowicz (1983). Except where noted in text, the contribution of light scattering to measured fluorescence of monomeric and heat-aggregated FITC-C9 solutions was less than 2% under the conditions used to measure anisotropy, as determined by direct measurement of the scattered components of emission using equivalent solutions of unlabeled C9 (monomer and heat polymerized). Limiting anisotropies (in the absence of macromolecular motion) were determined by extrapolation to infinite viscosity of Perrin plots derived for r measured in solutions of increasing viscosity (obtained by adding sucrose to buffer I).

The wavelength dependence of the steady-state anisotropy was determined by recording the polarized excitation spectra between 430 and 530 nm (2-nm slits), with the polarized emission (I_{VV}/I_{VH}) recorded at 560 nm (16 nm slits).

Fluorescence Lifetimes. Fluorescence lifetimes for samples equilibrated at 23 °C were determined by the phase (τ_p) and modulation (τ_m) techniques (δ-phase mode) using a modulating frequency of 30 MHz (Spencer & Weber, 1969; Spencer, 1970; Lakowicz et al., 1981; Lakowicz, 1983). Excitation was at 470 nm with a 0.5-nm slit, and emission was recorded at 520 nm (16-nm slit). To correct for effects due to sample polarization, excitation and emission polarizers were aligned at 0° and 54.7°, respectively (Spencer 1970; Lakowicz, 1983). When necessary, neutral density filters were added to match the intensities of sample and reference solutions. The scattered light from a dilute solution of oyster glycogen (measured at 470 nm) was used as a reference lifetime signal ($\tau_R = 0$ ns). Comparison to results obtained with a reference fluorophore (Me_2POPOP in absolute ethanol; $\tau_R = 1.45$ ns) confirmed that wavelength-dependent phase shifts of the photocurrent did not contribute appreciably to observed phase and modulation values between emission at 470 nm (measured for scattering reference) and emission at 520 nm (measured for FITC) under the experimental conditions (Lakowicz et al., 1981). A scattering reference was selected because of the small intensity of available reference lifetime fluorophores at the wavelengths employed for FITC (Lakowicz, 1983).

Results

Purification and FITC Labeling of C9. Complement protein C9 used for FITC labeling was isolated to biochemical and immunochemical purity as assessed by three criteria: (i) On polyacrylamide gel electrophoretic examination, the protein ran as a single homogeneous band of $M_r \sim 70\,000$. No impurities were detected by Coomassie staining. (ii) Immunochemical analysis of C9 performed on Ouchterlony plates revealed a single precipitin line when incubated against goat antiserum raised against the protein (Ouchterlony, 1968). No reactivity toward the protein was detected for antisera to human serum albumin, IgG, C7, C8, or whole human serum (see Materials and Methods). (iii) As measured in a standardized hemolytic assay employing C5b-8 erythrocytes, the

[3] Symbols: ϕ, fluorescence quantum yield; r, steady-state fluorescence anisotropy; τ_p, fluorescence lifetime calculated by phase method; τ_m, fluorescence lifetime calculated from measured fluorescence demodulation; τ_R, reference fluorophore lifetime; I_{VH}, fluorescence intensities measured for vertically (V) polarized excitation and horizontally (H) polarized emission. Vertical orientation of polarizers denotes 0° orientation in the laboratory frame of reference.

functional activity of the isolated protein was indistinguishable from that of pooled human serum, on the basis of an assumed normal serum C9 concentration of 58 μg/mL (Biesecker & Muller-Eberhard, 1980).

The selection of reaction conditions for FITC labeling of C9 was dictated by three specific considerations: (i) the presence of 40 lysines and the absence of free sulfhydryl groups on the native protein (Biesecker & Muller-Eberhard, 1980) and the existence of functionally important internal disulfides (Ware & Kolb, 1981; Yamamoto & Migita, 1983) which eliminated consideration of reagents with sulfhydryl reactivity, (ii) the requirement that the functional properties of the native protein be conserved and that reaction conditions leading to spontaneous polymerization of the molecule be avoided, and (iii) the requirement that labeling ratios of less than one to up to two FITC per protein be achieved and that the noncovalent adsorption of this hydrophobic chromophore to the protein be minimized (Maeda et al., 1969).

Preliminary trials employing FITC inputs of 1:1 to 10^4:1 (dye:protein), with reaction conditions that ranged from pH 7.5 to pH 9.0, suggested that satisfactory labeling, with minimal loss of functional activity, was achieved at pH 8.70, for FITC:C9 inputs of 10:1 to 200:1. Under these conditions, a labeling efficiency of 1–3% of input—with little reduction in C9 hemolytic activity—was routinely observed (see Materials and Methods).

Biochemical and Functional Properties of FITC-9. On examination by gel electrophoresis, FITC-C9 denatured in SDS was found to run as a single homogeneous band (as detected by protein staining) which exhibited an electrophoretic pattern identical with that of unlabeled C9 (data not shown). As detected by the measured fluorescence due to FITC eluted from unstained gel slices, >83% of the applied fluorescent label always comigrated with the protein band; the remainder was detected exclusively at the dye front. Since protein staining revealed no significant material at the dye front, these results suggest that a small component of the FITC associated with the labeled protein was noncovalently adsorbed. Attempts to elute this material from native FITC-C9 by either dialysis or chromatographic procedures were unsuccessful. On occasion, a small amount of high molecular weight material was detected on the top of the separating gel, suggesting aggregation of C9 during the labeling procedure. When detected, this material was readily separated from the FITC-C9 monomer by gel filtration on Sephacryl S-200 (see Materials and Methods).

As assessed by hemolytic activity toward C5b-8 SRBC (measured by the relative CH_{50}; see Materials and Methods), the FITC-C9 conjugates employed in this study (dye to protein ratios of 0.28 to 1.94) retained greater than 65% of the cytolytic function of native C9. At these labeling ratios, no correlation between the dye to protein ratio and the hemolytic activity was observed (data not shown), suggesting that the small reduction in hemolytic activity occasionally observed for FITC-C9 may be due to the reaction conditions employed for labeling (pH 8.70), rather than the incorporation of FITC into the protein per se.

Although results from hemolytic assay suggest that the fluoresceinated protein retains the biological activity of unlabeled C9, the possibility that the hemolytic activity observed for FITC-C9 resides exclusively in unlabeled molecules within a given preparation (e.g., 37% of those molecules labeled with an average dye/protein ratio of unity) cannot be excluded on the basis of the observed CH_{50}. Accordingly, the specific incorporation of FITC-C9 into membrane-associated C5b-9 was directly measured with C5b-8 treated-lipid vesicles as the

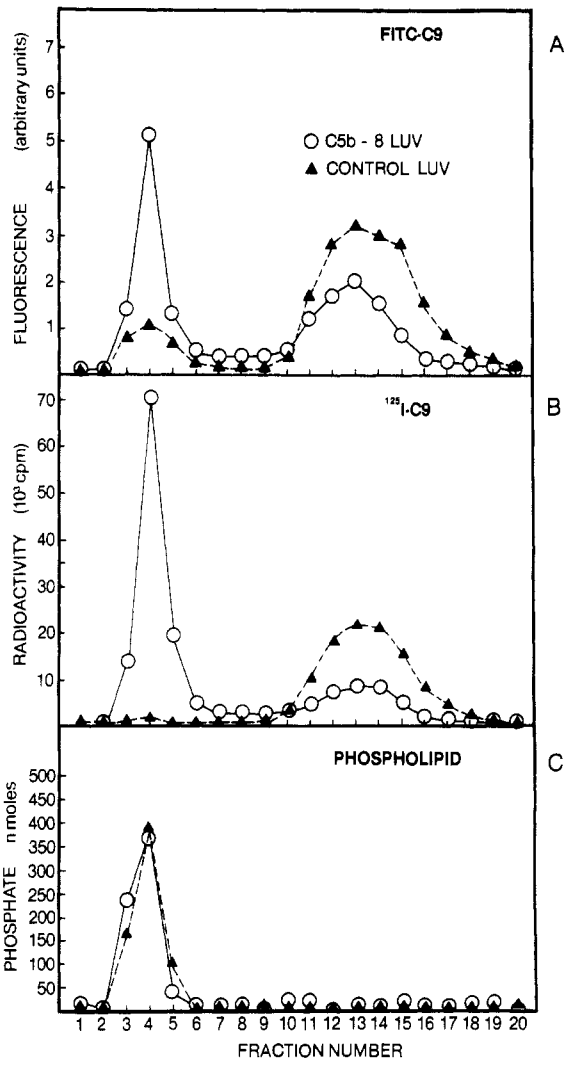

FIGURE 1: Binding of FITC-C9 to C5b-8 LUV as measured by discontinuous density gradient centrifugation. C5b-8 LUV and controls (0.6 mg of lipid) were each suspended with 23 μg of FITC-C9 (dye/protein ratio = 1.39) and 1.3 μg of ^{125}I-C9 (specific activity = 1.2×10^5 cpm/μg) in a total volume of 0.3 mL of buffer I. After incubation (30 min, 30 °C) vesicles were floated through a density gradient of Ficoll 70 as described under Materials and Methods. (A) Fluorescence of each fraction after dilution to 2.3 mL in buffer I. Excitation at 470 nm (4-nm slits); emission at 520 nm (4-nm slits). (B) Radioactivity (10^3 cpm). (C) Phosphate (nmol). Data shown for control LUV are similar to results obtained for C5b67 LUV suspended with FITC-C9 and ^{125}I-C9 in the absence of C8 (data not shown).

target membranes. In these experiments, large unilamellar egg phosphatidylcholine vesicles (LUV) were incubated with C5b6 + C7 and then suspended with C8 (unlabeled) and excess C9 trace labeled with both ^{125}I-C9 and FITC-C9. Following incubation, the LUV were separated from unbound protein by floatation on a discontinuous Ficoll 70 density gradient, according to the procedures described under Materials and Methods. As shown by the results presented in Figure 1, following centrifugation, 45–65% of the total initial fluorescence of the sample was removed from the bottom of the density gradients due to floatation of the C5b-8 vesicles, as compared to 8–15% found adsorbed nonspecifically to control LUV (Figure 1A). These data directly confirm the specific incorporation of FITC-C9 into the membrane-associated C5b-9 complex (MC5b-9). Comparison of the data obtained for FITC-C9 (Figure 1A) to those for ^{125}I-C9 (Figure 1B) reveals that the specific membrane binding of FITC-C9 (as measured by the reduction of fluorescence remaining at

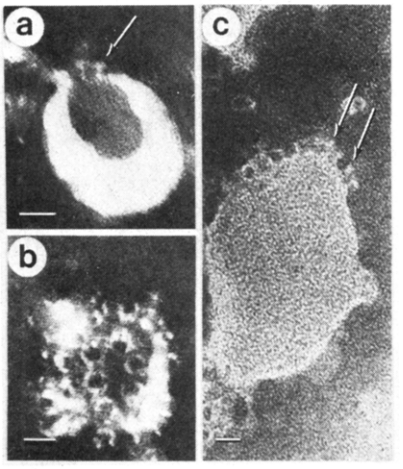

FIGURE 2: Ultrastructure of FITC-C9 incorporated into membrane-bound C5b-9 complex. Egg phosphatidylcholine unilamellar vesicles were exposed to complement proteins C5b-8 and FITC-C9 (dye to protein ratio = 1.94) and then examined by negative-stain electron microscopy (see Materials and Methods). In plates a and b, vesicles exhibiting typical 10 nm i.d. annulus-ringed cylinders can be seen projecting from membrane surface. In plate c, a row of complexes projecting from the surface can be viewed in profile (arrow). LUV shown in plate c were separated from unbound proteins by floatation through Ficoll 70 density gradient. Bar indicates 20-nm scale.

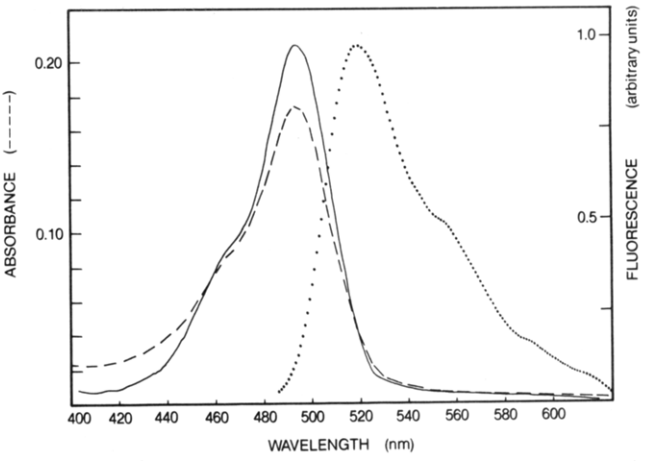

FIGURE 3: Visible absorbance, excitation, and emission spectra of FITC-C9 monomer. Visible wavelength absorbance (dashed line), fluorescence excitation (solid line), and fluorescence emission (dotted line) spectra for FITC-C9 monomer in buffer I. Corrected fluorescence excitation and emission spectra were obtained for 20 nM solution of FITC-C9 (dye/protein ratio = 1.21). Absorbance spectrum is for 2.4 μM solution of the same protein. For the fluorescence excitation spectrum, emission was recorded at 540 nm (8-nm slits) and excitation scanned at 1-nm intervals (1-nm slits). Corrections for lamp output, photomultiplier tube response, and sample polarization were made according to procedures described under Materials and Methods. Peak wavelength of absorbance and excitation spectra are 495 nm; peak emission wavelength was 519 nm.

the bottom of the density gradient) is 10–15% less than the specific uptake observed for ^{125}I-C9, which may suggest a small loss in activity of the fluoresceinated protein. Contributing to this apparent loss in C5b-8 specific membrane uptake of FITC-C9, however, is an increased nonspecific adsorption of FITC fluorescence (as compared to radioactivity), to control LUV (cf. Figure 1, parts A and B). Whether the fluorescence found associated with control LUV is due to the partition into membrane lipid of the small component of FITC adsorbed noncovalently to C9 (see above) or is due to an increased nonspecific adsorption of the labeled protein to control membranes (due, for example, to the hydrophobic nature of the conjugated chromophore) remains to be investigated.

Ultrastructural Properties of C5b-(FITC-)C9 LUV. In order to determine whether FITC-C9 retained the capacity to polymerize into the annulus-ringed cylinders that are characteristic of the structures formed by the native molecule when bound to C5b-8 membranes (Dourmashkin, 1978; Bhakdi & Tranum-Jensen, 1978; Podack et al., 1982), LUV treated with complement proteins C5b-8 + FITC-C9 [C5b-(FITC-)C9 LUV] were examined by negative-stain electron microscopy, before and after separation from unbound proteins by floatation on Ficoll 70. As is shown by Figure 2, FITC-C9 bound to C5b-8 LUV generated typical-10 nm i.d. annulus-ringed cylinders—which on cross section can be seen projecting from the membrane surface—that were indistinguishable from those observed after incubation of the C5b-8 LUV with unlabeled C9 (not shown). No C9 ring structures were observed after incubation at 30 °C of control LUV with either FITC-C9 or unlabeled C9 (data not shown). As has previously been reported for small unilamellar vesicles treated with the C5b-9 proteins (Tschopp et al., 1982a), LUV treated with the C5b-9 proteins (or with FITC-C9 substituted for C9) exhibited membrane fragmentation, aggregation, and fusion.

Spectral Properties of FITC-C9 (Monomer). In Figure 3 are presented the visible absorbance and the corrected visible excitation and emission spectra of monomeric FITC-C9 in buffer I (pH 7.50). The peak wavelength in the visible range of both the absorbance and excitation spectra recorded under these conditions was 495 nm, the peak emission observed at 519 nm (for excitation at 470 nm). The recorded spectra correspond closely to those previously reported for fluorescein conjugates of IgG and other proteins and exhibit the characteristic overlap of the fluorescein absorption and emission spectra (Weber, 1954; Chen, 1969; Wang & Taylor, 1980; Pick & Karlish, 1980).

Table I: Fluorescence Properties of FITC-C9 Monomer Labeled at Various Dye/Protein Ratios

dye/protein[a] ratio	ϕ[b]	r[c]	τ_p[d] (ns)	τ_m[e] (ns)
0.28	0.522	0.164 ± 0.001	3.83 ± 0.01	3.91 ● 0.02
0.33	0.495	0.164 ± 0.001	3.67 ± 0.04	3.72 ± 0.03
0.84	0.453	0.163 ± 0.001	3.72 ● 0.03	3.85 ● 0.06
1.21	0.405	0.161 ± 0.001	3.60 ± 0.02	4.02 ± 0.04
1.84	0.228	0.137 ● 0.002	3.55 ± 0.04	3.83 ± 0.01
1.94	0.313	0.140 ± 0.001	3.53 ● 0.003	3.81 ± 0.06

[a] Dye/protein ratios of FITC-C9 conjugates were determined on molar basis according to procedures described under Materials and Methods. [b] Quantum yield (ϕ) was determined for excitation at 495 nm. [c] Steady-state anisotropy (r) was measured (mean ± SD, n = 5) with excitation at 470 nm (4-nm slits) and emission at 520 nm (4-nm slits). [d] Lifetimes by phase (τ_p) and modulation (τ_m). See Materials and Methods.

The quantum yields (ϕ) of FITC-C9 conjugates were estimated to be 0.4–0.5 for labeling ratios (dye/protein) of less than unity but generally decreased to 0.2–0.3 as the labeling ratio approached 2:1 (Table I). Similarly, the steady-state anisotropy (r) measured for the monomeric protein in solution (excitation at 470 nm) varied inversely with the labeling ratio and was observed to drop sharply at labeling ratios approaching 2:1. At labeling ratios below unity, mean apparent fluorescence lifetimes of 3.7–3.9 ns were estimated for FITC bound to C9, with lifetimes estimated by the phase shift technique (τ_p) corresponding to within 3% of the lifetimes estimated on the basis of demodulation values (τ_m). As the labeling ratio exceeded unity, considerable deviation of calculated τ_p and τ_m were observed, suggesting the contribution of multiple lifetime

Table II: Fluorescence of FITC-C9 Bound to C5b-8 LUV[a]

sample	relative intensity[b]	r[c]	τ_p[d] (ns)	τ_m[d] (ns)
FITC-C9 (monomer)	(1.00)	0.161 ± 0.001	3.60 ± 0.02	4.02 ± 0.04
FITC-C9 + C5b-8 LUV	0.56	0.207 ± 0.001	3.43 ± 0.03	3.80 ± 0.03
isolated C5b-(FITC-)C9 LUV[e]		0.228 ± 0.003	3.40 ± 0.04	3.67 ± 0.07
miscellaneous controls				
FITC-C9 + LUV	1.07	0.163 ± 0.001	3.83 ± 0.08	3.82 ± 0.03
FITC-C9 + C5b67 LUV	1.03	0.168 ± 0.001	3.58 ± 0.02	3.58 ± 0.02
FITC-C9 + C8	0.95	0.160 ± 0.001	3.63 ± 0.02	3.95 ± 0.001
FITC-C9 + C8 + LUV	0.99	0.167 ± 0.001	3.67 ± 0.05	3.88 ± 0.07
FITC-C9 + C5b-8 LUV[f]	0.94	ND[g]	ND	ND

[a] Data are for 3 μg of FITC-C9 (dye/protein = 1.21) suspended in 2.1 mL of buffer I with 155 μg of egg phosphatidylcholine LUV treated with the various complement proteins indicated. Data for FITC-C9 monomer in solution are from Table I. Except where indicated, all samples were incubated at 30 °C for 30 min and then equilibrated at 23 °C before fluorescence was measured. [b] Fluorescence intensity (excitation 470 nm, emission 520 nm) normalized to that measured for FITC-C9 monomer in solution. [c] Steady-state anisotropy (r) measured with excitation at 470 nm (4-nm slits) and emission at 520 nm (4-nm slits). [d] Fluorescence lifetimes were obtained as described for Table I. [e] Vesicles were separated from unbound proteins by floatation on a discontinuous gradient of Ficoll 70 (see Materials and Methods). [f] FITC-C9 suspended with C5b-8 LUV at 2 °C. Sample fluorescence was measured at 2 °C and is expressed relative to fluorescence of FITC-C9 monomer equilibrated at the same temperature. [g] Not determined.

components to the fluorescence decay. In general, the mean lifetime calculated from both τ_p and τ_m decreased at labeling ratios above unity. Similar results have previously been reported for FITC-IgG (Chen, 1969).

Change in FITC-C9 Fluorescence upon Assembly of C5b-(FITC-)C9 LUV. As shown in Figure 4 and Table II incubation of FITC-C9 with C5b-8-treated vesicles resulted in a considerable decrease in total steady-state fluorescence, accompanied by a small red shift (1–3 nm) in the excitation and emission spectra. Comparison of the excitation spectra shown in Figure 4 for FITC-C9 monomer (solid trace) to that of FITC-C9 bound to C5b-8 LUV (dotted trace) reveals that the decrease of fluorescence observed upon binding to MC5b-8 is dependent upon excitation wavelength, the change in FITC-C9 fluorescence upon binding being less for excitation at the "red edge" (510–530 nm) of the FITC-C9 absorbance spectrum than at lower wavelengths. These data suggest that the reduction of FITC-C9 fluorescence which is observed upon binding to MC5b-8 depends upon the initial energy level of the excited state, the significance of which is considered below. No change in either the fluorescence excitation or emission spectra was observed when FITC-C9 was suspended with control LUV (in the absence of other proteins), control LUV + C8, C5b67 LUV (no C8), or C5b-8 LUV maintained and scanned at 2 °C (not shown; see also Table II). These data suggest that the change in FITC-C9 fluorescence observed upon incubation with C5b-8-treated vesicles is due to the specific activation of the molecule by membrane-associated C5b-8.

As recorded at 520 nm (excitation at 470 nm) steady-state fluorescence intensity upon the addition of excess C8 to C5b67 LUV + FITC-C9 decreased by 40–45% under optimal FITC-C9 to C5b-8 ratios. As is reported elsewhere (Sims & Wiedmer, 1984) both the rate and magnitude of the decrease in FITC-C9 fluorescence upon MC5b-9 assembly were observed to depend upon temperature, the C9 to C5b-8 ratio, and the composition of the target membranes.

As summarized by the data of Table II, following incubation of FITC-C9 with C5b-8 LUV, one observes a small increase in steady-state fluorescence anisotropy as compared to either the protein in solution or FITC-C9 suspended with control vesicles. In the absence of FITC-C9, no measureable change in light scattering was observed at the emission wavelength upon addition of C8 and C9 (unlabeled) to C5b67 vesicles (data not shown), suggesting that the observed change in anisotropy reflects a change in the properties of the chromophore upon FITC-C9 interaction with the C5b-8 membrane. The decrease in steady-state fluorescence upon FITC-C9 interaction with membrane C5b-8 is also accompanied by a small decrease in fluorescence lifetime, as determined by the phase shift method (Table II).

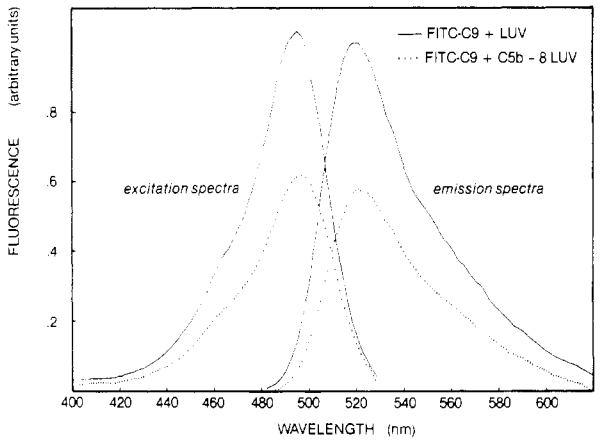

FIGURE 4: Change in FITC-C9 fluorescence upon incubation with C5b-8 LUV. Corrected visible wavelength fluorescence excitation and emission spectra for FITC-C9 (dye/protein = 1.21) after incubation (30 min, 30 °C) with either control LUV (solid lines) or C5b-8 LUV (dotted lines). Both samples contained 3 μg of FITC-C9 and 155 μg of lipid (LUV or C5b-8 LUV) in a total volume of 2.1 mL of buffer I. Samples were equilibrated at 23 °C before spectra were obtained. Spectra recorded under conditions described for Figure 3, with additional corrections made for light scattering due to vesicles (see Materials and Methods).

In order to confirm that the fluorescence changes recorded upon C8 addition to FITC-C9 + C5b-7 LUV suspensions were due specifically to the membrane binding of FITC-C9 (and not to a change in the physical properties of the unbound proteins), the steady-state anisotropy and fluorescence lifetimes were determined for FITC-C9 bound to C5b-8-treated LUV, after separation from unbound protein by floatation on Ficoll 70, according to methods previously described. As shown by the data of Table II, the steady-state fluorescence anisotropy and the fluorescence lifetime of FITC-C9 bound to isolated C5b-9 membranes corresponds to that observed for the FITC-C9 + C5b-8 LUV suspension, suggesting that the observed fluorescence change is due to assembly of membrane-bound C5b-(FITC-)C9 complexes.

Changes in Fluorescence Accompanying Heat Polymerization of FITC-C9. The quenching of FITC-C9 fluorescence upon formation of the membrane-bound C5b-(FITC-)C9

Table III: Fluorescence of Heat-Aggregated FITC-C9[a]

		dye/protein ratio	relative intensity	r	τ_p (ns)	τ_m (ns)
1	monomer	0.28	(1.00)	0.164 ± 0.001	3.83 ● 0.01	3.91 ± 0.02
	heat aggregated	0.28	0.65	0.089 ± 0.001	3.57 ± 0.04	3.83 ± 0.02
2	monomer	0.33	(1.00)	0.164 ● 0.001	3.67 ± 0.01	3.72 ● 0.03
	heat aggregated	0.33	0.43	0.068 ± 0.002	3.38 ± 0.07	3.33 ± 0.06
3	monomer	1.21	(1.00)	0.161 ± 0.001	3.60 ● 0.02	4.02 ± 0.04
	heat aggregated	1.21	0.78	0.109 ± 0.001	3.42 ± 0.05	3.60 ± 0.05
4	monomer	1.84	(1.00)	0.137 ± 0.002	3.55 ± 0.04	3.83 ± 0.01
	heat aggregated	1.84	0.42	0.080 ± 0.001	3.38 ● 0.09	3.57 ± 0.05
5	monomer	1.94	(1.00)	0.140 ● 0.001	3.53 ± 0.003	3.81 ± 0.06
	heat aggregated	1.94	0.37	0.058 ± 0.001	3.43 ± 0.01	3.23 ● 0.17

[a] FITC-C9 (dye to protein ratio = 0.28–1.94) was induced to polymerize by heating according to procedures described under Materials and Methods. Fluorescence of each sample was then measured and compared to matched-pair control samples (monomer) stored on ice. All fluorescence measurements were obtained with samples equilibrated at 23 °C according to procedures described for Table II. Anisotropy and lifetime data for FITC-C9 monomer controls are from Table I.

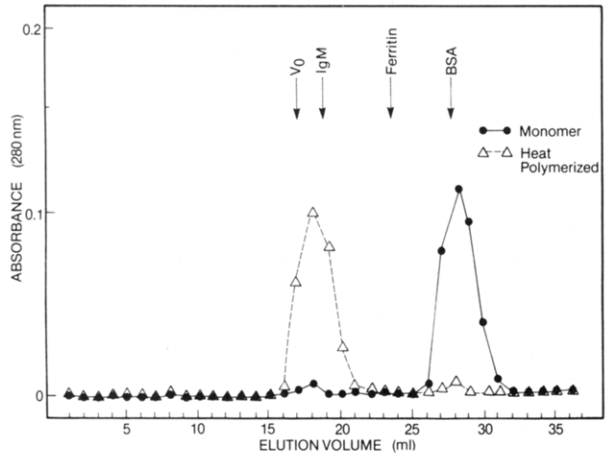

FIGURE 5: Molecular sieve chromatography of monomeric and heat-aggregated FITC-C9. FITC-C9 (dye/protein = 1.84) was chromatographed on Sephacryl S-300 (0.9 × 60 cm) before (solid trace) and after (dashed trace) heating to induce polymerization. Elution profiles obtained by measurement of sample fluorescence (excitation 470 nm; emission 520 nm; data not plotted) coincided with that shown for measured absorbance at 280 nm. Marker proteins bovine serum albumin, ferritin, and IgM eluted where indicated.

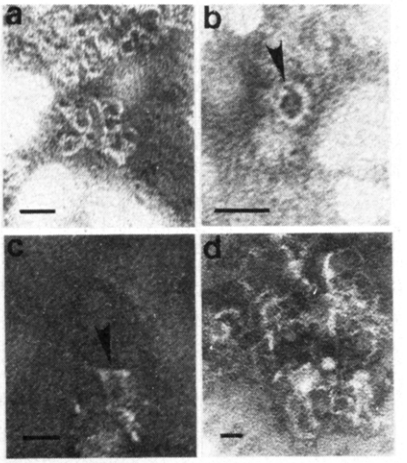

FIGURE 6: Ultrastructure of heat-polymerized FITC-C9 complex. Aggregates of FITC-C9 (dye to protein ratio = 1.84) were prepared by heating and then examined by negative-stain electron microscopy (see Material and Methods). In plates a and b, typical 10 nm i.d. ring forms can be seen on surface projection. Plate c shows the polymerized FITC-C9 cylinder as viewed in profile (arrow). In plate d, typical "strings" of polymerized protein are shown. Bars indicate 20-nm scale.

complex raises the possibilities that the chromophore is "reporting" the association of FITC-C9 with the C5b-8-treated membrane and/or the polymerization of the molecule into the activated C9 copolymer. In recent reports, it has been demonstrated that the self-association of C9 into "ringlike" and "beaded-string" aggregates can be induced either by heating the molecule or by chemical denaturation in guanidine (Podack & Tschopp, 1982a,b; Tschopp et al., 1982a; Dankert et al., 1983). Accordingly, the spectroscopic, biochemical, and ultrastructural properties of FITC-C9 following treatment to induce heat polymerization were investigated. As is shown by the data of Figure 5, incubation of FITC-C9 at 52 °C for 3 h often caused nearly complete aggregation of the protein, resulting in a polymer with an apparent molecular weight of greater than 10^6 (determined by gel filtration). These results are identical with those we have obtained for unlabeled C9 and with those previously reported for the molecule (Podack & Tschopp, 1982a,b; Tschopp et al., 1982a). It should be noted, however, that with certain preparations of serum C9 (either unlabeled or FITC conjugated) we were unable to detect significant polymerization of the molecule following prolonged heating at either 37 or 52 °C. Furthermore, among various preparations of C9 (and FITC-C9), we observed no correlation between the hemolytic activity of the protein and its capacity for heat-induced polymerization under these conditions (data not shown). Similar observations have recently been made by Esser and associates (Dankert et al., 1983).

Electron microscopic examination of FITC-C9 following heat treatment revealed the presence of diverse structural forms that included occasional annulus-ringed cylinders, previously described for polymerized C9 (Podack & Tschopp, 1982a,b; Tschopp et al., 1982a), as well as elongated "strings" of protein and large aggregates of indistinct structure (Figure 6). The ultrastructural appearance of heat-treated FITC-C9 was indistinguishable from that observed for heat-treated C9 (unlabeled). No aggregate "ring" or "string" forms were observed by electron microscopy for monomeric FITC-C9 controls (not shown).

In Figure 7 and Table III are summarized the fluorescence properties of heat-polymerized FITC-C9. Polymerization of the protein typically results in a large decrease in total fluorescence intensity and a small red shift of the excitation and emission spectra of the fluorophore. Qualitatively, these results are identical with those observed for FITC-C9 upon its binding to C5b-8 LUV membranes. As noted for FITC-C9 bound to C5b-8 LUV (Figure 4), inspection of the excitation spectra for the monomeric and heat-polymerized forms of FITC-C9 reveals that the quenching of fluorescence observed upon aggregation of the molecule can virtually be eliminated

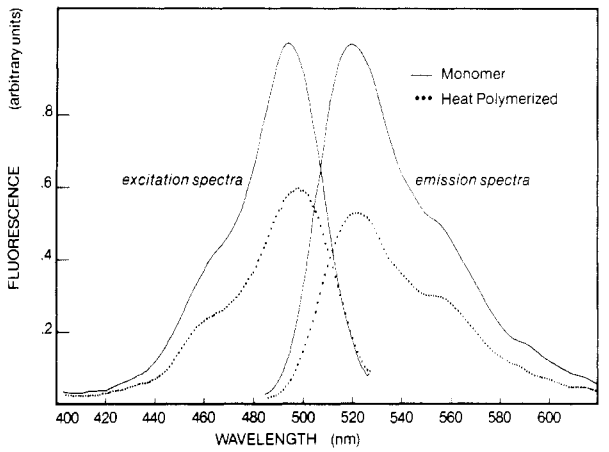

FIGURE 7: Change in FITC-C9 fluorescence upon heat-induced aggregation. Corrected visible fluorescence excitation and emission spectra are shown for FITC-C9 monomer control (solid line) and heat-induced polymer (dotted line). Each sample contained 6 μg of FITC-C9 (dye/protein = 1.84) in 2.5 mL of buffer I. Spectra were recorded and corrected as previously described (see legend to Figure 3).

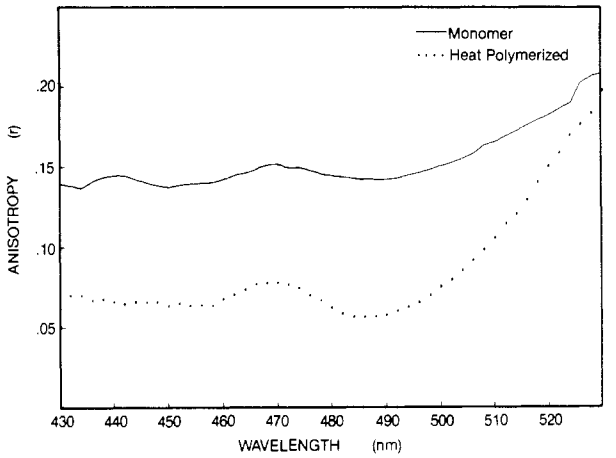

FIGURE 8: Effect of excitation wavelength on steady-state anisotropy measured for heat aggregated FITC-C9. Steady-state anisotropy (r) as derived from excitation polarization spectra of FITC-C9 monomer (solid trace) and heat-induced polymer (dotted trace). Samples were prepared as described for Figure 7 (dye/protein = 1.84), and polarized excitation spectra obtained as described under Materials and Methods. Steady-state anisotropy was calculated according to eq (2).

by exciting on the red edge (510–530 nm) of the absorbance spectrum (see Figure 7). For some preparations of FITC-C9, heat-induced polymerization resulted in a reduction of the steady-state fluorescence (excitation at 470 nm) by more than 60%, exceeding the degree of quenching (generally less than 50%; see above) that was observed for FITC-C9 binding to C5b-8 LUV. Upon heat-induced polymerization, the visible absorbance spectrum of FITC-C9 typically exhibited a 1–2-nm red shift of the absorbance maximum, with only a small decrease in peak absorbance (always less than 10%). It should also be noted, that for certain preparations of heat-polymerized FITC-C9, no change in the visible absorbance spectrum could be discerned, despite a large decrease in the steady-state fluorescence of the molecule, suggesting that fluorescence quenching is due in large part to excited-state processes (see below).

In contrast to the increase in steady-state anisotropy observed upon FITC-C9 binding to C5b-8 LUV (cf. Table II), upon heat-induced polymerization, FITC-C9 invariably showed a large decrease in steady-state fluorescence anisotropy, accompanied by a small decrease in the apparent fluorescence lifetime (Table III). These changes in fluorescence anisotropy and lifetime observed for the protein in solution upon heat-induced polymerization are qualitatively similar to the trends observed for each of these parameters at labeling ratios (dye/protein) exceeding unity (cf. Table I). As shown by the data of Figure 8, the steady-state anisotropy observed for the polymerized form of FITC-C9 depended upon the excitation wavelength, with the aggregation-induced depolarization of emission being virtually eliminated when the chromophore was excited on the low energy (red edge) of its absorbance spectrum.

Mechanism of FITC-C9 Quenching upon C5b-9 Assembly. The similarity of the steady-state emission and excitation spectra recorded for FITC-C9 bound to C5b-8 membranes (Figure 4) to those recorded following heat-induced polymerization of the molecule in a lipid-free system (Figure 7) suggests that the observed quenching of the molecule results from the self-aggregation of FITC-C9 on the C5b-8 membrane surface, rather than the binding of FITC-C9 monomers to the membrane per se. This interpretation is particularly suggested by our failure to observe quenching (or red shifting) of FITC-C9 emission upon incubation with C5b-8 vesicles at 2 °C, a temperature at which the molecule is known to reversibly bind to the membrane but not exhibit pore forming activation (Alving et al., 1980; Okada et al., 1980; Sims & Wiedmer, 1984).

Possible mechanisms for FITC-C9 quenching upon copolymerization include (i) self energy transfer between neighboring fluoresceins (Forster, 1948; Weber, 1954) due to the considerable overlap of the absorption and emission spectra of the fluorophore (see Figures 3, 4, and 7), (ii) static complex formation or collisional self-quenching between multiple fluoresceins on the adjacent FITC-C9, (iii) quenching of FITC fluorescence by tryptophan or other aromatic residues on the same or adjacent proteins (Watt & Voss, 1977), and (iv) a conformational change in the protein which occurs upon activation by C5b-8 and membrane insertion—or upon heat-induced polymerization—which results in a change in the environment of the pH-sensitive fluorescein chromophore (Martin, 1975; Martin & Lindqvist, 1975).

The decrease in both quantum yield and anisotropy observed for multiple FITC substitution of the monomeric protein (Table I)—and indirect evidence for the existence of heterogeneous lifetime components contributing to the fluorescence decay ($\tau_p \neq \tau_m$; cf. Tables I–III)—suggest that self energy transfer between FITC located on adjacent C9 monomers might account for the fluorescence changes recorded following FITC-C9 binding to C5b-8 LUV, as well as for those observed upon heat-induced polymerization of the molecule. This interpretation is also suggested by the dependence upon excitation wavelength observed for fluorescence quenching (and depolarization) in the aggregated state of FITC-C9, both of which can be virtually eliminated by excitation at the low-energy edge of the absorbance spectrum (cf. Figures 4, 7, and 8). Fluorescein to fluorescein energy transfer within a heterogeneous population of chromophores is expected to result in a decrease in net fluorescence intensity (due to sequential energy transfer to lower energy excited states with increased probability of radiationless decay) and to result in depolarization of the steady-state fluorescence [due to electronic transfer through multiple absorption and emission dipoles before observed photon emission; see Forster (1948), Weber (1954), Weber (1966), Dale & Bauer (1971), and Lakowicz (1983)]. Elimination of these effects by red-edge excitation of fluorescein has previously been described by Weber & Shinitzky (1970) and Dale & Bauer (1971).

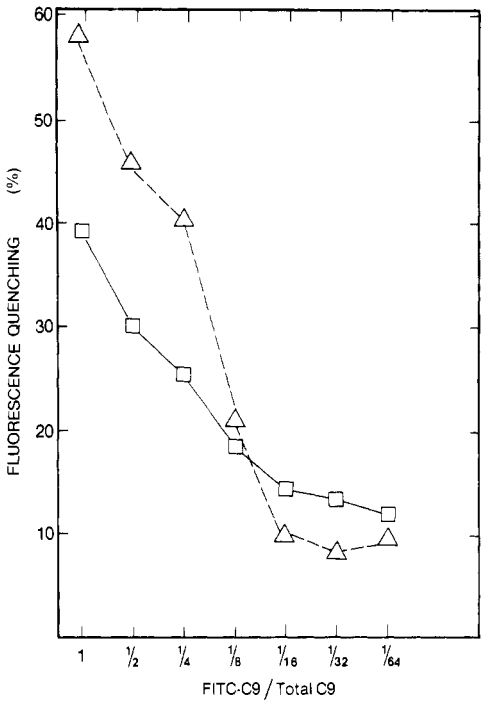

FIGURE 9: Fluorescence quenching due to FITC-C9 polymerization and binding to MC5b-8: effect of dilution by unlabeled C9. The quenching of FITC-C9 fluorescence (ordinate) measured for heat-polymerized FITC-C9 (△) and FITC-C9 incubated with C5b-8 LUV (□) in the presence of various amounts of unlabeled C9. The ratio of FITC-C9/total C9 (abscissa) was varied by equimolar substitution of FITC-C9 (dye/protein ratio = 1.84) by unlabeled C9, maintaining total C9 in each sample constant (see text). Fluorescence quenching for each sample (heat-polymerized FITC-C9 or FITC-C9 + C5b-8 LUV suspension) is expressed as the percent decrease from the fluorescence (excitation 470 nm; emission 520 nm) of matched-pair control samples (unheated FITC-C9 monomers or FITC-C9 + C5b67 LUV suspensions, respectively) prepared at identical FITC-C9/total C9 ratios. Data are corrected for measured light scattering from aggregated protein and/or vesicles as described under Materials and Methods.

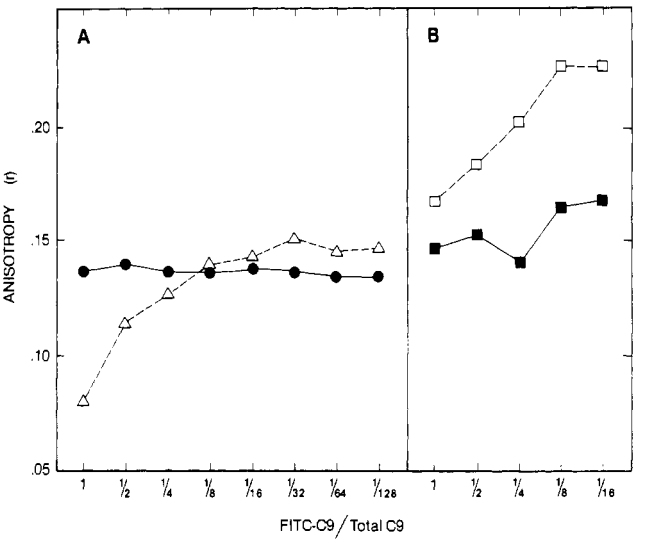

FIGURE 10: Effect of FITC-C9/total C9 ratio upon fluorescence anisotropy of polymerized FITC-C9 and membrane-bound FITC-C9. (Panel A) Emission anisotropy (r) of FITC-C9 monomers (●) and heat-induced polymers (△) prepared at various FITC-C9/total C9 ratios (abscissa) as described for Figure 9. (Panel B) Emission anisotropy (r) of FITC-C9 after incubation with C5b67 LUV controls (■) or C5b-8 LUV (□) at various FITC-C9/total C9 ratios under conditions described for Figure 9. All measurements were made at 23 °C in buffer I with excitation at 470 nm (4-nm slits) and emission at 520 nm (16-nm slits). Steady-state anisotropy was calculated from the parallel (I_{VV}) and perpendicular (I_{VH}) components of emission, after correction for measured light scattering due to proteins and/or vesicles, as described under Materials and Methods. Dye/protein ratio of FITC-C9 used for both experiments was 1.84.

In order to directly demonstrate that energy transfer *between* adjacent FITC-C9 monomers contributes to the fluorescence changes observed for the polymerized protein, the quenching of fluorescein fluorescence upon heat-induced polymerization of the molecule and that upon FITC-C9 binding to C5b-8 LUV were each measured under conditions in which the ratio of FITC-C9 to total C9 was systematically varied (keeping total C9 input constant) by equimolar substitution of C9 (unlabeled) for FITC-C9. As shown by the data of Figure 9, as the ratio of FITC-C9 to total C9 was decreased (by substitution with unlabeled C9), the extent of fluorescence quenching measured either upon heat-induced polymerization or upon binding to C5b-8 LUV decreased significantly. Since one-for-one substitution of FITC-C9 by unlabeled C9 is not expected to alter either the conformation of the labeled protein or the environment of the fluorophore (after C9 activation and polymerization)—but will reduce the likelihood that two FITC residues will be bound to adjacent C9 monomers—these results suggest a mechanism of self-quenching involving intermolecular energy transfer that can occur either upon FITC-C9 activation by MC5b-8 (leading to membrane localization of the C9 copolymer) or upon heating (forming polymeric aggregates in solution).

Additional evidence for excited-state energy transfer upon FITC-C9 activation and polymerization was obtained by measuring the effect of the FITC-C9/total C9 ratio upon the fluorescence anisotropy measured when the protein is induced to aggregate in solution (Figure 10A) and after its activation and binding to MC5b-8 (Figure 10B). As previously described (see Table III and Figure 8) in the absence of unlabeled C9 (FITC-C9/total C9 ratios near unity) heat-induced polymerization of the protein causes a significant decrease in anisotropy (for excitation at 570 nm), despite a 10–15-fold increase in macromolecular size (Figure 5). Since protein aggregation would normally be expected to increase anisotropy (assuming constant lifetime) due to retarded motional freedom of the chromophore (see Discussion), the observed decrease in r upon polymerization suggests an intervening depolarizing process (e.g., resonance energy transfer). This likelihood is confirmed by the data of Figure 10A, which demonstrate that upon dilution of FITC-C9 by unlabeled C9 (total C9 input constant) the anisotropy of the protein in the polymerized state *increases*. Furthermore, at FITC-C9/total C9 ratios below 1/8 to 1/16, polymerization of the protein results in an increase in measured steady-state anisotropy to values significantly *higher* than that measured for the monomer in solution. In these experiments, the steady-state anisotropy of the unaggregated monomers remained virtually constant during FITC-C9 dilution by the unlabeled protein (Figure 10A), suggesting that inner filter effects did not contribute significantly to these measurements.

For FITC-C9 bound to C5b-8 LUV (Figure 10B) one-for-one dilution by unlabeled C9 resulted in an increase in the measured anisotropy to values considerably higher than that observed for the undiluted labeled protein, suggesting that the observed anisotropy of MC5b-8-bound FITC-C9 is also diminished by the depolarizing effects of self-transfer (see Discussion). It should be noted, however, that in the experiments of Figure 10B, accurate determination of anisotropy at high dilutions of the labeled protein was technically limited by the increase in the relative contribution of light scattering at measuring wavelengths by membrane vesicles under these conditions. The contribution of scattered light to these

data—despite our efforts to correct for these effects (see Materials and Methods)—is suggested by the slight increase in anisotropy measured for controls at high dilution of FITC-C9 (solid squares, Figure 10B).

Discussion

The data of recent reports provide considerable evidence that the polymerization of C9 and the concomitant unfolding of hydrophobic domains within the molecule are the key molecular events that initiate cytolytic membrane damage by the serum complement proteins: (i) In the absence of C9, C5b-8-treated cells exhibit only subtle changes in permeability, resulting in a prolonged lytic phase (Stolfi, 1968; Ramm et al., 1982b). The addition of C9 dramatically increases the lytic efficiency of the complement system, reducing by orders of magnitude the number of membrane-bound C5b-8 complexes required to observe an increase in membrane permeability (Sims, 1983). (ii) Ultrastructural studies have shown that the annulus-ringed tubules (doughnut holes) found on the membranes of complement-lysed cells are formed by copolymers of C9 arranged in a cylindrical array, and evidence has been presented that the C5b-8 proteins form a separate membrane-associated complex which is distinct from the putative C9 membrane pore (Tschopp et al., 1982a,b; Podack & Tschopp, 1982a,b). (iii) Data obtained by photoaffinity labeling with membrane-restricted probes suggest that a hydrophobic domain of C9 is the major protein structure intercalated into the hydrocarbon region of lipid bilayers, with the remaining C5b-8 proteins largely inaccessible to labeling by reagents localized near the center of the bilayer (Hu et al., 1981; Ishida et al., 1982; Steckel et al., 1983). (iv) Studies with C9 in solution demonstrate its potential for spontaneous polymerization, which is accompanied by increased hydrophobic properties and evidence for increased β-sheet structure within the protein (Podack & Tschopp, 1982a,b; Tschopp et al., 1982a,b). Evidence for the membranolytic potential of this polymerized form of C9 has been considered (Tschopp & Podack, 1981; Tschopp et al., 1982a).

In the present report, we demonstrate that the event of C9 polymerization—either spontaneously in solution, or upon activation and membrane insertion at the C5b-9 pore site—can be directly monitored by measuring the steady-state fluorescence of an FITC derivative of the protein. Additionally, we have demonstrated that this change in fluorescence observed upon FITC-C9 polymerization is due in large part to intermolecular resonance energy transfer (RET) between FITC chromophores in the aggregated poly(C9) complex.

The evidence for self energy transfer upon FITC-C9 polymerization includes (i) the virtual elimination of fluorescence quenching (and depolarization) upon FITC-C9 aggregation that is observed for excitation at the low-energy red edge (510–530 nm) of the absorbance spectrum (Figures 4, 7, and 8), (ii) anomalous depolarization of the steady-state fluorescence upon polymerization of the labeled protein in solution (Table III and Figures 8 and 10A), and (iii) the relationship of fluorescence quenching (and steady-state anisotropy) in the polymerized state to the ratio of labeled to unlabeled C9 (Figures 9 and 10), suggesting that the close proximity of FITC chromophores is essential for the change in fluorescence observed upon C9 aggregation.

In considering how the polymerization of FITC-C9—with the resulting potential for energy transfer between FITC on neighboring C9 monomers—will alter the steady-state anisotropy (r) measured for the chromophore, it is important to emphasize that multiple dynamic processes contribute to the observed polarization of the steady-state fluorescence. First, it is reasonable to assume that upon aggregation of C9 monomers, segmental motions of the protein (and/or rotational freedom of the attached chromophore) will be sterically hindered. By restriction of depolarizing motion during the lifetime of the excited state, polymerization of the protein will therefore tend to increase the observed steady-state anisotropy. In the case of the membrane-inserted protein complex [MC5b-(FITC-)C9], further constraints upon the depolarizing motion of the attached chromophore can be anticipated, with the mobility of membrane-inserted peptides now presumably restricted to a wobble about the axis normal to the membrane plane. On the other hand, the potential for RET between neighboring fluoresceins within the polymerized FITC-C9 complex will cause depolarization of the steady-state fluorescence (decreasing anisotropy) due to randomization of absorption and emission dipoles through multiple conjugated excited states (Weber, 1966; Chen, 1969; Dale & Bauer, 1971; Lakowicz, 1983). Thus, it can be assumed that in the case of polymerized FITC-9 in solution (Table III), the depolarization of fluorescence due to RET between fluoresceins on clustered FITC-C9 monomers dominates the observed steady-state anisotropy, obscuring any increase arising due to hindered rotational relaxation of the chromophore in the aggregated structure. Only when RET is effectively precluded—either by excitation to the low-energy state resulting from the 0–0 transition on the red edge of the absorbance spectrum (Figure 8) or by interspacing unlabeled C9 within the polymerized protein complex (Figure 10A)—is the anticipated increase in steady-state anisotropy due to protein aggregation observed. The dependence of the transfer depolarization of fluorescein upon chromophore proximity ("concentration depolarization") and excitation energy (the red-edge effect) has previously been analyzed by Weber (1954), Weber & Shinitzky (1970), and Dale & Bauer (1971).

In the case of the membrane-inserted complex, the small increase in anisotropy observed upon MC5b-8 binding and activation of FITC-C9 (Table II and Figure 10B) can be attributed to severe constraints upon depolarizing motion expected for the membrane-inserted C5b-9 protein complex, the effects of which are offset in part by the depolarizing effect of self-transfer which occurs between clustered FITC-C9 monomers. In this context it should be noted that the small increase in r often observed for FITC-C9 bound to C5b-8 membranes was considerably smaller than that measured under conditions restricting the potential for energy transfer between bound FITC-C9 monomers (i.e., at low FITC-C9/total C9 ratios; see Figure 10B). It is of interest that under these conditions (low FITC-C9/total C9 ratios) the steady-state anisotropy observed for membrane-bound FITC-C9 approaches a value ($r \simeq 0.23$; Figure 10B) significantly higher than that observed for the heat-aggregated protein ($r \simeq 0.15$; Figure 10A) under comparable limiting conditions of reduced transfer depolarization. On the basis of these results, one might speculate that the motional freedom of the chromophore within the membrane-bound C5b-9 complex is more restricted than it is within the heat-induced C9 polymer, suggesting conformational and/or environmental differences between these two forms of aggregated C9 (see above). In interpreting these data, however, it is necessary to caution that definitive conclusions about the conformational or motional properties of the chromophore in these two forms of C9 (heat aggregated and MC5b-8 bound) are precluded by the uncertainty of whether residual transfer depolarization (due to RET between multiple FITC on the same or adjacent C9 monomers) contributes to the anisotropy measured under these conditions (see

Table I). The effect of light scattering on these measurements has been discussed (see Results). Future studies with chromophores better suited for an evaluation of the motional properties of the bound protein are planned.

From the data of Figures 9 and 10, it would appear that the fluorescence self-quenching and self-transfer depolarization which occur either in the heat-aggregated FITC-C9 complex or for FITC-C9 bound to C5b-8 membranes can each be substantially eliminated by dilution of the labeled protein (with unlabeled C9) to ratios generally exceeding 1/8 to 1/16 (FITC-C9/total C9). These results suggest that in both forms of the polymerized protein, a similar relationship of the probability for FITC self-transfer to the intermolecular spacing of unlabeled C9 monomers pertains. Whether this is directly related to the number of C9 monomers that combine per unit C9 copolymer (estimated by electron microscopy to be approximately 12; Tschopp et al., 1982a,b) or to transfer probabilities that are not directly related to intermolecular spacing (e.g., orientation between donor and acceptor chromophores) requires further study.

To summarize, we have demonstrated that FITC-C9 substantially retains the functional, biochemical, and ultrastructural properties of the unlabeled protein, including its capacity to interact with membrane-bound C5b-8 to generate the cytolytic membrane lesion. Furthermore, we have presented evidence that the fluorescence quenching of this probe upon membrane assembly is specifically related to the molecular event of C9 polymerization at the C5b-9 pore site. We therefore believe that this fluorescent derivative of C9 provides a novel spectroscopic tool by which to dynamically probe the molecular events that occur upon the activation and assembly of the cytolytic complement proteins on membrane surfaces. Furthermore, because fluorescein is well suited to measurements in biological systems (using conventional optics provided with fluorescence microscopes and fluorescence-activated cell sorters), we believe this probe may find application in studies with living cells, in addition to basic studies employing model membranes.

Acknowledgments

The helpful comments and suggestions of Drs. Joseph Eisinger, Alfred F. Esser, Richard P. Haugland, Joseph R. Lakowicz, Thomas E. Thompson, Thomas W. Tillack, and Therese Wiedmer are gratefully acknowledged. I wish especially to thank Dr. J. R. Lakowicz for generously sharing unpublished manuscripts. Certain reagents used in the purification of the complement proteins were generous gifts from Dr. A. F. Esser and The Biological Laboratories of the Department of Public Health, Boston, MA. The superb technical assistance of Paul Dean, Judith Piros, and Ellen Boswell is gratefully acknowledged, as is the generous assistance of Margaretta Allietta in the preparation of electron micrographs. Finally, I wish to acknowledge the patient and skillful assistance of Peggy Snow and Melinda Mills in preparation of the manuscript.

Registry No. Complement C9, 80295-59-6; complement C5b-9, 82986-89-8; fluorescein isothiocyanate, 27072-45-3.

References

Alving, C. R., Urban, K. A., & Richards, R. L. (1980) *Biochim. Biophys. Acta 600*, 117.

Bartlett, G. R. (1959) *J. Biol. Chem. 234*, 466.

Bhakdi, S., & Tranum-Jensen, J. (1978) *Proc. Natl. Acad. Sci. U.S.A. 75*, 5655.

Biesecker, G., & Muller-Eberhard, H. J. (1980) *J. Immunol. 124*, 1291.

Bull. W. H. O. (1968) *39*, 935.

Chen, R. F. (1969) *Arch. Biochem. Biophys. 133*, 263.

Dale, R. E., & Bauer, R. K. (1971) *Acta Phys. Pol. A A40*, 853.

Dankert, J. R., Shiver, J. W., Mason, E. R., & Esser, A. F. (1983) *Fed. Proc., Fed. Am. Soc. Exp. Biol. 42*, 1773.

Dourmashkin, R. R. (1978) *Immunology 35*, 205.

Duzgunes, N., Wilshut, J., Hong, K., Fraley, R., Perry, C., Friend, S., James, T. L., & Papahadjopoulos, D. (1983) *Biochim. Biophys. Acta 732*, 289.

Esser, A. F. (1981) in *Biological Membranes* (Chapman, D., Ed.) pp 277–322, Academic Press, New York.

Esser, A. F., Kolb, W. P., Podack, E. R., & Muller-Eberhard, H. J. (1979) *Proc. Natl. Acad. Sci. U.S.A. 76*, 1410.

Forster, T. H. (1948) *Ann. Phys. (Leipzig) 2*, 55.

Hammer, C. H., Wirtz, G. H., Renfer, L., Gresham, H. D., & Tack, B. F. (1981) *J. Biol. Chem. 256*, 3995.

Hu, V. W., Esser, A. F., Podack, E. R., & Wisnieski, B. J. (1981) *J. Immunol. 127*, 380.

Ishida, B., Wisnieski, B. J., Lavine, C. H., & Esser, A. F. (1982) *J. Biol. Chem. 257*, 10551.

Jackson, R. J., Mendelein, J., & Sachs, G. (1983) *Biochim. Biophys. Acta 731*, 9.

Laemmli, U. K. (1970) *Nature (London) 227*, 680.

Lakowicz, J. R. (1983) *Principles of Fluorescence Spectroscopy*, Plenum Press, New York.

Lakowicz, J. R., Cherek, H., & Balter, A. (1981) *J. Biochem. Biophys. Methods 5*, 131.

Maeda, J., Ishida, N., Kawauchi, H., & Tuzimuro, K. (1969) *J. Biochem. (Tokyo) 65*, 777.

Martin, M. M. (1975) *Chem. Phys. Lett. 35*, 105.

Martin, M. M., & Lindqvist, L. (1975) *J. Lumin. 10*, 381.

Mayer, M. M. (1972) *Proc. Natl. Acad. Sci. U.S.A. 69*, 2954.

Michaels, D. W., Abramovitz, A. S., Hammer, C. H., & Mayer, M. M. (1976) *Proc. Natl. Acad. Sci. U.S.A. 73*, 2852.

Monahan, J. B., Stewart, J. L., & Sodetz, J. M. (1983) *J. Biol. Chem. 258*, 5056.

Muller-Eberhard, H. J. (1975) *Annu. Rev. Biochem. 44*, 697.

Okada, M., Boyle, M. D. P., & Borsos, T. (1980) *Biochem. Biophys. Res. Commun. 94*, 406.

Ouchterlony, O. (1968) *Handbook of Immunodiffusion and Immunoelectrophoresis*, Ann Arbor Scientific Publications, Ann Arbor, MI.

Pick, U., & Karlish, S. J. D. (1980) *Biochim. Biophys. Acta 626*, 255.

Podack, E. R., & Tschopp, J. (1982a) *Proc. Natl. Acad. Sci. U.S.A. 79*, 574.

Podack, E. R., & Tschopp, J. (1982b) *J. Biol. Chem. 257*, 15204.

Podack, E. R., Tschopp, J., & Muller-Eberhard, H. J. (1982) *J. Exp. Med. 156*, 268.

Ramm, L. E. Whitlow, M. B., & Mayer, M. M. (1982a) *Proc. Natl. Acad. Sci. U.S.A. 79*, 4751.

Ramm, L. E., Whitlow, M. B., & Mayer, M. M. (1982b) *J. Immunol. 129*, 1143.

Shinitzky, M. (1972) *J. Chem. Phys. 56*, 5979.

Shinitzky, M., Dianoux, A.-C., Gitler, C., & Weber, G. (1971) *Biochemistry 10*, 2106.

Sims, P. J. (1983) *Biochim. Biophys. Acta 732*, 511.

Sims, P. J., & Lauf, P. K. (1978) *Proc. Natl. Acad. Sci. U.S.A. 75*, 5669.

Sims, P. J., & Wiedmer, T. (1984) *Biochemistry* (following paper in this issue).

Spencer, R. D. (1970) Ph.D. Thesis, University of Illinois at Urbana–Champagne.

Spencer, R. D., & Weber, G. (1969) *Ann. N.Y. Acad. Sci. 158*, 361.
Steckel, E. W., Wellbaum, B. E., & Sodetz, J. M. (1983) *J. Biol. Chem. 258*, 4318.
Stolfi, R. (1968) *J. Immunol. 100*, 46.
Stryer, L. (1978) *Annu. Rev. Biochem. 47*, 819.
Szoka, F., & Papahadjopoulos, D. (1980) *Annu. Rev. Biophys. Bioeng. 9*, 467.
Tschopp, J., & Podack, E. R. (1981) *Biochim. Biophys. Res. Commun. 100*, 1409.
Tschopp, J., Muller-Eberhard, H. J., & Podack, E. R. (1982a) *Nature (London) 298*, 534.
Tschopp, J., Podack, E. R., & Muller-Eberhard, H. J. (1982b) *Proc. Natl. Acad. Sci. U.S.A. 79*, 7474.
Wang, Y.-L., & Taylor, D. L. (1980) *J. Histochem. Cytochem. 28*, 1198.
Ware, C. F., & Kolb, W. P. (1981) *Proc. Natl. Acad. Sci. U.S.A. 78*, 6426.
Watt, R. M., & Voss, E. W., Jr. (1977) *Immunochemistry 14*, 533.
Weber, G. (1954) *Trans. Faraday Soc. 50*, 552.
Weber, G. (1966) in *Fluorescence and Phosphorescence Analysis* (Hercules, D. D., Ed.) pp 217–240, Wiley, New York.
Weber, G., & Shinitzky, M. (1970) *Proc. Natl. Acad. Sci. U.S.A. 65*, 823.
Yamamoto, K.-I., & Migita, S. (1983) *J. Biol. Chem. 258*, 7887.

Kinetics of Polymerization of a Fluoresceinated Derivative of Complement Protein C9 by the Membrane-Bound Complex of Complement Proteins C5b-8†

Peter Jay Sims* and Therese Wiedmer

ABSTRACT: The fluorescence self-quenching by energy transfer of FITC-C9, a fluoresceinated derivative of human complement protein C9 [Sims, P. J. (1984) *Biochemistry* (preceding paper in this issue)], has been used to monitor the kinetics of C9 polymerization induced by the membrane-associated complex of complement proteins C5b-8. Time-based measurements of the fluorescence change observed during incubation of FITC-C9 with C5b-8-treated sheep red blood cell ghost membranes at various temperatures revealed that C9 polymerization induced by the C5b-8 proteins exhibits a temperature dependence similar to that previously reported for the complement-mediated hemolysis of these cells, with an Arrhenius activation energy for FITC-C9 polymerization of 13.3 ± 3.2 kcal mol^{-1} (mean ± 2 SD). Similar measurements obtained with C5b-8-treated unilamellar vesicles composed of either egg yolk phosphatidylcholine (egg PC), dipalmitoylphosphatidylcholine (DPPC), or dimyristoylphosphatidylcholine (DMPC) revealed activation energies of between 20 and 25 kcal mol^{-1} for FITC-C9 polymerization by C5b-8 bound to these membranes. Temperature-dependent rates of C9 polymerization were observed to be largely unaffected by the phase state of membrane lipid in the target C5b-8 vesicles. The significance of these observations to the mechanism of C9 activation of membrane insertion is considered.

Cytolytic membrane damage by the serum complement system is initiated upon the association of component C9 with membrane-bound complexes formed of complement proteins C5b, C6, C7, and C8 (Muller-Eberhard, 1975; Esser, 1982; Bhakdi & Tranum-Jensen, 1983).[1] It has recently been demonstrated that the incorporation of C9 into the membrane-bound C5b-8 complex (MC5b-8) results in the copolymerization of multiple molecules of C9 and the exposure of hydrophobic domains within the protein (Podack & Tschopp, 1982; Tschopp et al., 1982; Podack et al., 1982b). Under conditions promoting disulfide exchange, interchain disulfide bonds are formed that can covalently link C9 monomers in the polymerized C9 complex (Ware & Kolb, 1981; Yamamoto & Migita, 1983). By intercalating through bilayer lipid, tubules of polymerized C9 are thought to initiate a change in membrane permeability that leads to the collapse of ionic gradients and consequent cell death (Tschopp et al., 1982).

Considerable insight into the mechanism of membrane damage by these key immunoproteins has been derived from ultrastructural analysis of the membrane-bound C5b-9 complex and from biochemical studies of the association of the proteins either in solution or following extraction from detergent-solubilized membranes [reviewed by Esser (1982), Tschopp et al. (1982), and Bhakdi & Tranum-Jensen (1983)]. Additionally, analysis of the temperature dependence of complement-mediated hemolysis and measurements of the rates of diffusion of various solutes across C5b-9 damaged membranes have provided clues to the molecular events preceding cell lysis [reviewed by Boyle & Borsos (1980) and Esser (1982)]. Nevertheless, a direct kinetic analysis of the terminal molecular event that is presumed to initiate functional membrane damage—the MC5b-8 catalyzed activation and polymerization of C9 monomers—has not previously been possible, due to the inability to directly measure the self-association of

† From the Immunohematology Laboratory, the Department of Pathology (P.I.S. and T.W.), and the Department of Biochemistry (P.J.S.), University of Virginia School of Medicine, Charlottesville, Virginia 22908. *Received November 15, 1983.* This research was supported by a grant-in-aid from the American Heart Association with funds contributed in part by the Virginia Affiliate and by a grant from the Thomas F. Jeffress and Kate Miller Jeffress Memorial Trust. P.J.S. is a John A. Hartford Foundation Fellow. T.W. was supported by NIH Grant GM-26894. A preliminary account of this work was presented at the 28th Meeting of the Biophysical Society, San Antonio, TX, Feb 19–23, 1984.

[1] Complement proteins are named in accordance with recommendations of *Bull W. H. O.* (1968). The prefix "M" (e.g., MC5b-8) is used to indicate that the protein is membrane associated. EAC1–9 refers to an antibody-treated erythrocyte treated with complement proteins C1–C9.

0006-2960/84/0423-3260$01.50/0